HHS Public Access

Author manuscript

Neurogastroenterol Motil. Author manuscript; available in PMC 2023 February 01.

Published in final edited form as:

Neurogastroenterol Motil. 2022 February ; 34(2): e14292. doi:10.1111/nmo.14292.

Whole gut imaging allows quantification of all enteric neurons in the adult zebrafish intestine

Wael N. El-Nachef[1,2], **Claire Hu**[2], **Marianne E. Bronner**[2]

[1]Department of Medicine, Vatche and Tamar Manoukian Division of Digestive Diseases, University of California Los Angeles

[2]Division of Biology and Biological Engineering, California Institute of Technology

Abstract

Background: A fundamental understanding of the enteric nervous system in normal and diseased states is limited by the lack of standard measures of total enteric neuron number. The adult zebrafish is a useful model in this context as it is amenable to *in toto* imaging of the intestine. We leveraged this to develop a technique to image and quantify all enteric neurons within the adult zebrafish intestine and applied this method to assess the relationship between intestine length and total enteric neuron number.

Methods: Dissected adult zebrafish intestines were immunostained in wholemount, optically cleared with refractive index matched solution, and then imaged in tiles using light sheet microscopy. Imaging software was used to stitch the tiles, and the full image underwent automated cell counting. Total enteric neuron number was assessed in relation to intestinal length using linear regression modelling.

Results: Whole gut imaging of the adult zebrafish intestine permits the visualization of endogenous and immunohistochemistry-derived fluorescence throughout the intestine. While enteric neuron distribution is heterogeneous between intestinal segments, total enteric neuron number positively correlates with intestinal length.

Conclusions: Imaging of all enteric neurons within the adult vertebrate intestine is possible in models such as the zebrafish. Here, we apply this to demonstrate a positive correlation between enteric neuron number and intestine length. Quantifying total enteric numbers will facilitate future studies of enteric neuropathies and ENS structure in animal models and potentially in biopsied tissue samples.

INTRODUCTION

Several gastrointestinal diseases are categorized as enteric neuropathies, which often implies a loss of enteric neurons. In the case of Hirschsprung Disease, observing a complete absence of neurons within a segment of the colon may be technically simple to confirm[1]. However,

Correspondence: Marianne Bronner, PhD, California Institute of Technology, MC 139-74, 1200 E. California Blvd, Pasadena, CA 91125, mbronner@caltech.edu, Phone: 626-395-3358.

Disclosures:
All authors report no conflicts to disclose

in other conditions, such as gastroparesis, the role of enteric neuron loss as the pathologic lesion is less clear[2]. This is due in part to limitations of quantifying enteric neurons from a small sample and then extrapolating to the whole organ. Indeed, normal ranges of enteric neuron number determined by extrapolation-based methods vary widely, and such practices have been unambiguously discouraged due to lack of consistent reproducibility[3]. Reliably quantifying enteric neuronal numbers is a basic biologic measure that could greatly enhance our fundamental understanding of several gastrointestinal diseases.

Animal models for gastrointestinal diseases have proven crucial for understanding disease ontogeny and progression. The zebrafish is a vertebrate model organism increasingly recognized for its applicability to and advantages for gastroenterological research[4]. Because the typical adult zebrafish is 2–3 cm, imaging the adult intestine *in toto* is technically feasible, especially when compared to other common vertebrate models whose intestines are significantly longer and thicker in the adult stages.

To enable accurate quantification of neuronal numbers, we have developed a method to image the full length of the adult zebrafish intestine that permits visualization of all enteric neurons which can then be submitted for automated cell counting. We applied this method to assess the relationship between total enteric neuron number and intestine length, uncovering a positive correlation. This technique is well suited for applications related to enteric neuropathies and enteric nervous system architecture.

MATERIALS AND METHODS

Zebrafish

Adult zebrafish (Danio rerio) were maintained at 28°C and on a 13-hour light/11-hour dark cycle. All zebrafish work was completed in compliance with the California Institute of Technology Institutional Animal Care and Use Committee. Ten adult AB wildtype male zebrafish aged 12 months and originating from the same clutch were included in this study. Zebrafish were euthanized with ice cold water, and measurement of body length (distance from the snout to the caudal peduncle) was made with a ruler.

Intestine Harvesting

Dissections occurred in the morning prior to initial feeding, thus the fish were in a fasting state. The intestine (sans esophagus and anus) was removed intact, placed in a petri dish in its native S-shape configuration, kept moist with approximately 1 mL of 1x PBS, and then imaged with a Zeiss Stemi SV11 microscope with an attached Zeiss Axiocam MRc digital camera. Photomicrographs of the intestine were later analyzed with the ImageJ software (National Institutes of Health) ruler function to determine intestinal length.

After photomicrographs were obtained, the intestine underwent further dissection of the connective tissue that maintain its S-shape configuration such that it ultimately took the shape of a straight tube. Then, a 10 μL pipette tip was ensheathed by the intestine [Fig. 1A] to maintain its shape during overnight fixation in 4% paraformaldehyde in 0.1M phosphate buffer at 4°C. Intestines were harvested serially on the same day.

Immunohistochemistry

After fixation, the intestines were removed from the pipette tips and washed with 1x PBS, then placed in blocking solution (2% goat serum, 1% bovine serum albumin, 1% DMSO, 0.1% Triton X-100 and 0.05% Tween 20 in 1x PBS) for 2 h at room temperature. Intestines were then incubated in primary antibody (anti-HuC/D IgG2b 1:200; Thermo Fisher Scientific A21271) diluted in blocking solution overnight at room temperature and washed for 2 h to 3 h in 1x PBS plus 0.1% Triton X-100. Then, samples were incubated overnight in secondary antibody (goat anti-mouse IgG2b 647 1:500, Thermo Fisher Scientific A21242) diluted in blocking solution overnight at room temperature and washed for 2–3 h in 1x PBS plus 0.1% Triton X-100.

Optical Clearing and Mounting

To achieve optical clearing, intestines were submerged in refractive index matching solution (RIMS)[5] for 48 hours at 4°C. The mounting medium was 1.5% low-melt agarose (IBI scientific, IB70056) prepared in RIMS. The cleared intestine was submerged into the melted mounting medium and then aspirated into a 1 mL syringe (BD, ref 309659) that had its tip cut off. Forceps were used to finalize positioning of the intestine within the syringe to optimize a linear orientation. This RIMS-based mounting medium maintained optical clearing of the intestine [Fig. 1A’].

Light Sheet Microscopy

The Zeiss Z.1 Light dual side illumination sheet fluorescence microscope was utilized in this study. The syringe containing the cleared intestine was loaded into the microscope, and then the syringe plunger was used to suspend the mounted intestine into an imaging chamber filled with RIMS. Imaging was performed using Zen software with LSFM module. Images were obtained with 5x objectives with an NA of 0.16, with a Z step of 5.760 μm. To image the entire intestine, image tiles were collected with 10% overlap to facilitate stitching.

Image Processing and Analysis

Tile images were manually stitched using Imaris Stitcher x64 v9.6.0 (Bitplane). The stitched image was then submitted for automated cell counting using the “Spots” feature on Imaris x64 v9.6.0 (Bitplane). Statistical analysis was performed using GraphPad Prism 8.2.1 (GraphPad Software, Inc). Correlations of intestinal length vs body length and total enteric neuron number vs intestinal length were assessed using linear regression modelling. R^2 values were used to report goodness of fit, and slopes were considered significantly non-zero if $p < 0.05$.

Imaging Endogenous Fluorescence

Intestines from adult zebrafish of the Phox2b^{kaede} transgenic line Tg(−8.3bphox2b:Kaede)[6] were prepared as above, except they did not undergo staining for immunohistochemistry.

RESULTS

Cleared intestines are compatible with *in toto* imaging of immunohistochemistry and endogenous fluorescence.

After whole mount immunostaining with HuC/D, adult zebrafish intestine imaged with light sheet microscopy demonstrated numerous neuronal nuclei [Fig. 1B]. Luminal views of the imaged intestine confirmed maintenance of three-dimensional cylindrical structure. Endogenous fluorescence was also preserved with this technique, as demonstrated in intestines originating from Phox2b^{kaede} fish. Stitching of tiled images permitted the creation of an *in toto*, three-dimensional image of the adult intestine, revealing dense circumferential and longitudinal neuronal projections [Fig 1C].

Enteric neuron density varies within the intestinal tract.

Adult zebrafish intestines were stained for HuC/D to facilitate counting of neuronal nuclei throughout the intestine [Fig. 2A]. Enteric neuron counts within 300 μm^2 varied significantly by intestinal segment, with higher neuronal concentrations in the distalmost hindgut versus the proximal end of the foregut (116.1 versus 63.80, p=0.0008) [Fig. 2B], and varied within segments amongst the fish (hindgut range 72–175 neurons [SD 35.90], foregut range 31–98 [SD 19.90]). Manual and automated cell counts (10 samplings of 300 μm^2) did not demonstrate a statistically significant difference (p=0.9156) [Fig. 2C], which was further supported by Bland-Altman analysis with all measurements falling within the 95% limits of agreement [Fig. 2D].

Total enteric neuron number positively correlates with intestine length.

We applied this technique to 10 adult male ABWT zebrafish originating from the same clutch but of differing body lengths. In humans, the length of the intestine is roughly proportional to height[7], but it is unknown if longer intestines contain proportionally more enteric neurons. We found that there is a significant correlation between zebrafish body length and intestinal length ($R^2 = 0.50$, $p = 0.022$) [Fig. 2E]. Total number of enteric neuronal nuclei ranged from 6,414 to 15,506 (mean = 10,448.9; SD = 2857.8) and positively correlated with intestinal length ($R^2 = 0.74$, $p = 0.0014$) [Fig. 2F].

DISCUSSION

Our technique of whole gut imaging is convenient and effective, and quantifies total enteric neuron number without relying on extrapolation. Previous estimations of enteric neuronal numbers in zebrafish were reported in the range of 400–750 neurons per square millimeter[8], though it is unclear how to best translate this measure to total enteric neuronal numbers. Furthermore, as apparent on our whole gut imaging, the distribution of neurons is not homogeneous, thus raising the issue of sampling errors if extrapolating from small sections. As demonstrated in multiple studies in mammals[9–13], tissue clearing is typically performed in sections or segments of intestine, which again is limited to extrapolation of enteric neuronal numbers. Moreover, such studies may require more time-consuming and intensive protocols with active clearing techniques or the use of other clearing agents which can distort the natural anatomy and/or ablate endogenous fluorescence[14].

During embryogenesis, enteric neurons arise from the vagal neural crest, and development in zebrafish is generally stereotypical during these early time points. Determinants of final body length in the adult, though, are multifactorial and include environmental conditions such as population density, water quality, and diet[15]. Body length correlates with intestinal length, which suggests intestinal length may also be influenced by such factors. Our results support a positive association between intestine length and total enteric neuron number in vertebrates, which has not been directly demonstrated previously. If intestinal length influences total enteric neuron number, it is unclear when or from which source these additional neurons arise. Whole gut imaging can be leveraged to explore the potential of enteric neurogenesis in post-embryonic stages.

In addition, given the simplicity of this technique, whole gut imaging facilitates higher-throughput comparative quantitative analyses rather than descriptive studies consisting of a few samples. If applied to models of gastrointestinal disease, this technique can also assess if presumed enteric neuropathies indeed result in reduced numbers of neurons or neuronal subtypes in the intestinal tract.

Lastly, our technique allows preservation of endogenous fluorescence and tissue structure using a relatively simple method of tissue clearing which can aid studies of cellular architecture of the enteric nervous system and associated cell types across the entire intestine.

ACKNOWLEDGEMENTS

We thank the Beckman Institute Biological Imaging Facility of Caltech for technical assistance with microscopy experiments. We thank the Ian Shepherd Lab for generously sharing the Tg(−8.3bphox2b:Kaede) line. We also recognize Phia Honey for technical assistance with sample preparation. Competing interests: the authors have no competing interests.

Grant Support:

This work was supported by the National Institutes of Health (NIH R35NS111564 to M.E.B., NIH R01NS108500 to M.E.B., and NIH K08DK123387 to WNE).

DATA AVAILABILITY STATEMENT

The data that support the findings of this study are available from the corresponding author upon reasonable request.

REFERENCES

1. Heuckeroth RO. Hirschsprung disease - integrating basic science and clinical medicine to improve outcomes. Nat Rev Gastroenterol Hepatol 2018;15:152–167. [PubMed: 29300049]
2. Grover M, Farrugia G, Lurken MS, et al. Cellular changes in diabetic and idiopathic gastroparesis. Gastroenterology 2011;140:1575–1585.e8. [PubMed: 21300066]
3. Knowles CH, Veress B, Kapur RP, et al. Quantitation of cellular components of the enteric nervous system in the normal human gastrointestinal tract--report on behalf of the Gastro 2009 International Working Group. Neurogastroenterol Motil 2011;23:115–124. [PubMed: 21175997]
4. Ganz J Gut feelings: Studying enteric nervous system development, function, and disease in the zebrafish model system. Dev Dyn 2018;247:268–278. [PubMed: 28975691]

5. Yang B, Treweek JB, Kulkarni RP, et al. Single-cell phenotyping within transparent intact tissue through whole-body clearing. Cell 2014;158:945–958. [PubMed: 25088144]
6. Harrison C, Wabbersen T, Shepherd IT. In vivo visualization of the development of the enteric nervous system using a Tg(−8.3bphox2b:Kaede) transgenic zebrafish. Genesis 2014;52:985–990. [PubMed: 25264359]
7. Raines D, Arbour A, Thompson HW, et al. Variation in small bowel length: factor in achieving total enteroscopy? Dig Endosc 2015;27:67–72. [PubMed: 24861190]
8. Uyttebroek L, Shepherd IT, Harrisson F, et al. Neurochemical coding of enteric neurons in adult and embryonic zebrafish (Danio rerio). J Comp Neurol 2010;518:4419–4438. [PubMed: 20853514]
9. Yuan P-Q, Bellier J-P, Li T, et al. Intrinsic cholinergic innervation in the human sigmoid colon revealed using CLARITY, three-dimensional (3D) imaging, and a novel anti-human peripheral choline acetyltransferase (hpChAT) antiserum. Neurogastroenterol Motil 2020:e14030. [PubMed: 33174295]
10. Bossolani GDP, Pintelon I, Detrez JD, et al. Comparative analysis reveals Ce3D as optimal clearing method for in toto imaging of the mouse intestine. Neurogastroenterol Motil 2019;31:e13560. [PubMed: 30761698]
11. Fu Y-Y, Peng S-J, Lin H-Y, et al. 3-D imaging and illustration of mouse intestinal neurovascular complex. Am J Physiol Gastrointest Liver Physiol 2013;304:G1–11. [PubMed: 23086917]
12. Liu Y-A, Chen Y, Chiang A-S, et al. Optical clearing improves the imaging depth and signal-to-noise ratio for digital analysis and three-dimensional projection of the human enteric nervous system. Neurogastroenterol Motil 2011;23:e446–457. [PubMed: 21895876]
13. Graham KD, López SH, Sengupta R, et al. Robust, 3-Dimensional Visualization of Human Colon Enteric Nervous System Without Tissue Sectioning. Gastroenterology 2020;158:2221–2235.e5. [PubMed: 32113825]
14. Liu CY, Polk DB. Cellular maps of gastrointestinal organs: getting the most from tissue clearing. Am J Physiol Gastrointest Liver Physiol 2020;319:G1–G10. [PubMed: 32421359]
15. Singleman C, Holtzman NG. Growth and Maturation in the Zebrafish, Danio Rerio: A Staging Tool for Teaching and Research. Zebrafish 2014;11:396–406. [PubMed: 24979389]

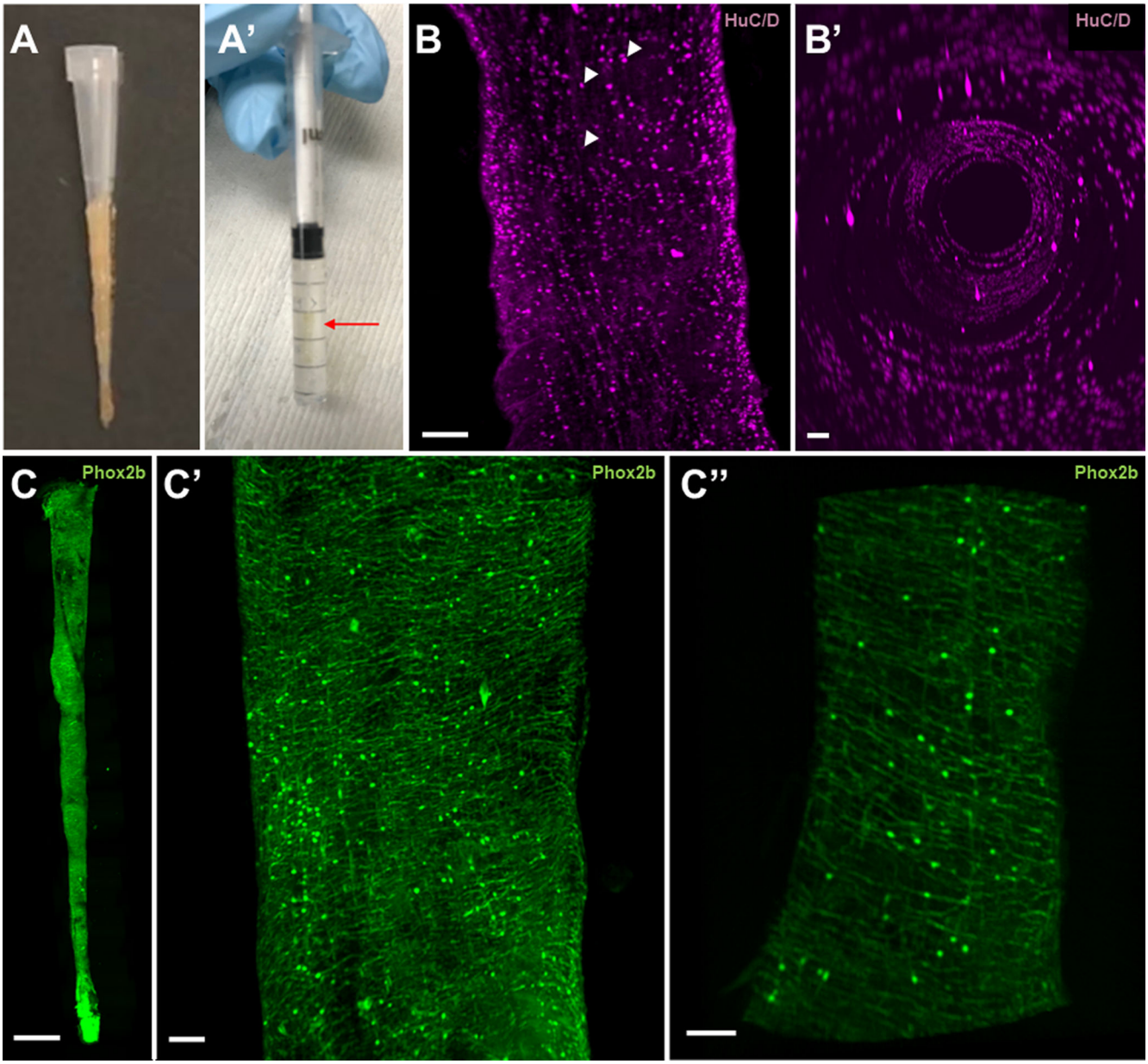

Figure 1: Optically cleared intestine preserves 3D structure and endogenous fluorescence to reveal a dense neural network throughout the adult zebrafish intestine.

1A) An adult zebrafish intestine before and after optical clearing. After harvesting the intestine, the connective tissue that maintains the organ in an S-shape configuration is further dissected, leaving a straight conical structure. Application of a pipette tip prevents tissue distortion during the fixation process (A). A cleared adult intestine within a 1 mL syringe that has been mounted with low-melt agarose prepared in RIMS (A'). Although difficult to visualize, the intestine (red arrow) is oriented longitudinally within the syringe.

1B) A two-dimensional projected image of the distal hindgut immunostained for HuC/D, which recognizes neuronal nuclei, demonstrates distinct nuclei without cellular projections (B). Arrowheads indicate representative nuclei at various Z-levels. Luminal view of the intestine highlights the three-dimensional quality of the imaging methods (B').

1C) The final stitched image (two-dimensional projection of the Z-stack) of the entire intestinal tube of an adult Phox2b^{kaede} zebrafish, which marks enteric neurons. At this magnification, it is not possible to discern individual neurons or their projections (C). A close-up of the midgut, which is again a two-dimensional projection of the Z-stack, reveals numerous neurons with dense projections spanning circumferentially as well as longitudinally (C'). A longitudinal optical section through the tangential edge of the midgut demonstrates the distribution of neurons in the intestine (C").
Scale bar 100um

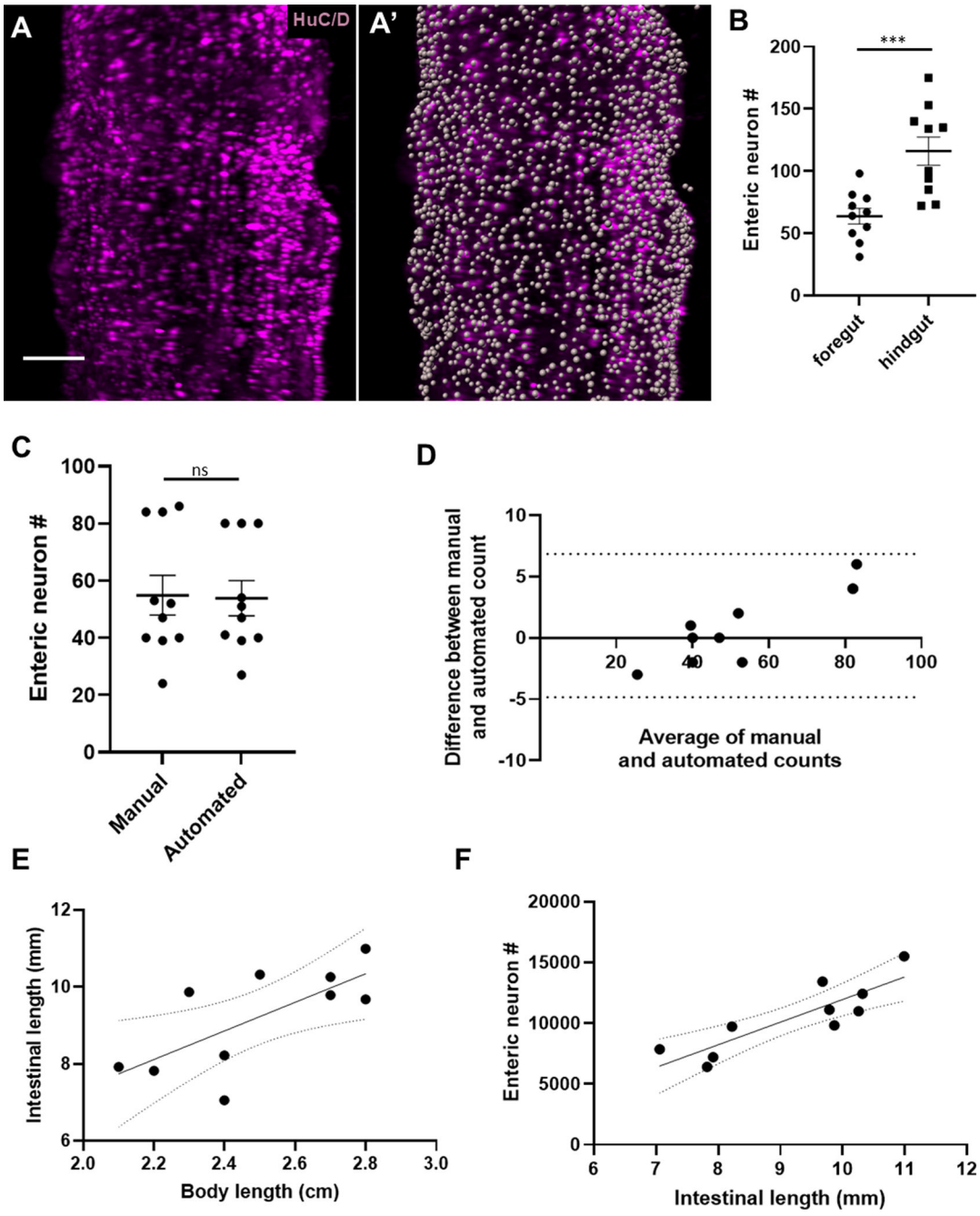

Figure 2: Whole gut imaging with immunostaining versus HuC/D reveals varied density of neurons within the intestine and proportional increase of total neuron number relative to intestinal length.

2A) Representative image of a segment of hindgut immunostained for HuC/D before (A) and after (A') automated cell counting.

2B) Cell counts within 300 μm^2 revealed significantly higher densities of neurons in the distal hindgut versus the proximal foregut (116.1 vs 63.80, p=0.0008).

2C and 2D) Manual and automated cell counts within 300 μm^2 sample regions (N=10) were not significantly different by T test analysis (p=0.9156) [Fig. 2C]. Agreement between

automated and manual counts was further supported by Bland-Altman analysis, with all measurements falling within the 95% limits of agreement (dotted lines) [Fig. 2D].
2E) A linear regression analysis of intestinal length vs body length ($R^2 = 0.50$, $p = 0.022$), with dotted lines representing the 95% confidence interval.
2F) A linear regression analysis of enteric neuron number versus intestinal length ($R^2 = 0.74$, $p = 0.0014$), with dotted lines representing the 95% confidence interval.
Scale bar 100um